A Non-homogeneous Time Mixed Integer LP Formulation for Traffic Signal Control

Iain Guilliard
National ICT Australia
7 London Circuit
Canberra, ACT, Australia
iguilliard@nicta.com.au

Scott Sanner
Oregon State University
1148 Kelley Engineering Center
Corvallis, OR 97331
scott.sanner@oregonstate.edu

Felipe W. Trevizan
National ICT Australia
7 London Circuit
Canberra, ACT, Australia
felipe.trevizan@nicta.com.au

Brian C. Williams
Massachusetts Institute of Technology
77 Massachusetts Avenue
Cambridge, MA 02139
williams@csail.mit.edu

5738 words + 7 figures + 1 tables + 23 citations (Weighted total words: 7738 out of 7000 + 35 references)
July 29, 2015

ABSTRACT

We build on the body of work in mixed integer linear programming (MILP) approaches that attempt to jointly optimize traffic signal control over an *entire traffic network* (rather than focus on arterial routes) and specifically on improving the scalability of these methods for large urban traffic networks. Our primary insight in this work stems from the fact that MILP-based approaches to traffic control used in a receding horizon control manner (that replan at fixed time intervals) need to compute high fidelity control policies only for the early stages of the signal plan; therefore, coarser time steps can be employed to "see" over a long horizon to preemptively adapt to distant platoons and other predicted long-term changes in traffic flows. To this end, we contribute the queue transmission model (QTM) which blends elements of cell-based and link-based modeling approaches to enable a non-homogeneous MILP formulation of traffic signal control. We then experiment with this novel QTM-based MILP control in a range of networks demonstrating the improved scalability possible with non-homogeneous time steps in comparison to the best homogeneous time step. Our experiments also provide near-optimal traffic control policies for larger horizons and larger networks than shown in previous implementations of MILP-based traffic signal control.

Using 204 words up to here. Maximum is 250 words.

[1]

[1]Make sure to follow instructions and author guide: http://onlinepubs.trb.org/onlinepubs/AM/InfoForAuthors.pdf http://onlinepubs.trb.org/onlinepubs/am/2015/WritingForTheTRRecord.pdf

Also note this example related paper from Steve Smith (formatted to TRB specs): https://www.ri.cmu.edu/pub_files/2014/1/TRB14UTC.pdf

INTRODUCTION

As cities rapidly grow in population while urban traffic infrastructure often adapts at a slower pace, it is critical to maximize capacity and throughput of existing road infrastructure through optimized traffic signal control. Unfortunately, many large cities still use some degree of *fixed-time* control (e.g., Toronto (*1*)) even if they also use *actuated* or *adaptive* control methods such as SCATS (*2*) or SCOOT (*3*). However, there is further opportunity to improve traffic signal control even beyond adaptive methods through the use of *optimized* controllers as evidenced in a variety of approaches ranging from mixed integer (linear) programming (*4, 5, 6, 7, 8, 9*) to heuristic search (*10, 11*) to scheduling (*12*) to reinforcement learning (*1*). While such optimized controllers hold the promise of maximizing existing infrastructure capacity by finding more complex (and potentially closer to optimal) jointly coordinated intersection policies than arterially-focused master-slave approaches such as SCATS and SCOOT, such optimized methods are computationally demanding and either (a) do not guarantee jointly optimal solutions over a large intersection network (often because they only consider coordination of neighboring intersections or arterial routes) or (b) fail to scale to large intersection networks simply for computational reasons (which is the case for many mixed integer programming approaches).

In this work, we build on the body of work in mixed integer linear programming (MILP) approaches that attempt to jointly optimize traffic signal control over an *entire traffic network* (rather than focus on arterial routes) and specifically on improving the scalability of these methods for large urban traffic networks. In our investigation of existing approaches in this vein, namely exemplar methods in the spirit of (*6, 8, 9*) that use a (modified) cell transmission model (CTM) (*13, 14*) for their underlying prediction of traffic flows, we remark that a major drawback is the CTM-imposed requirement to choose a predetermined homogeneous (and often necessarily small) time step for reasonable modeling fidelity. This need to model large number of CTM cells with a small time step leads to MILPs that are exceedingly large and intractable to solve.

Our primary insight in this work stems from the fact that MILP-based approaches to traffic control used in a receding horizon control manner (that replan at fixed time intervals) need to compute high fidelity control policies only for the early stages of the signal plan; therefore, coarser time steps can be employed to "see" over a long horizon to preemptively adapt to distant platoons and other predicted long-term changes in traffic flows. This need for non-homogeneous control in turn spawns the need for an additional innovation: we require a traffic flow model that permits non-homogeneous time steps and properly models the travel time delay between lights. To this end, we might consider CTM extensions such as the variable cell length CTM (*15*), stochastic CTM extensions (*16, 17*), extensions for better modeling freeway-urban interactions (*18*) including CTM hybrids with link-based models (*19*), assymmetric CTMs for better handling flow imbalances in merging roads (*20*), the situational CTM for better modeling of boundary conditions (*21*), and the lagged CTM for improved modeling of the flow density relation (*22*). However, despite the widespread varieties of the CTM and the usage of the CTM (*23*) for a range of applications, there seems to be no extension that permits non-homogeneous time steps as required in our novel MILP-based control approach.

For this reason, as a major contribution of this work to enable our non-homogeneous time MILP-based model of joint intersection control, we contribute the queue transmission model (QTM) which blends elements of cell-based and link-based modeling approaches with the following key benefits:

- unlike previous joint intersection control work (*6, 8, 9*), it is inherently intended for *non-homogeneous* time steps that can be used for control over large horizons,
- any length of roadway with no merges or diverges can be modeled as a single queue leading to compact models of large traffic networks thus maintaining relatively compact MILPs for large traffic networks (i.e., larges numbers of cells are not required between intersections), and
- it accurately models fixed travel time delays critical to green wave coordination as in (*4, 5, 7*) through the use of a non-first order Markovian update[2] model and combines this with the more global intersection signal optimization approach of (*6, 8, 9*).

In the remainder of this paper, we first formalize our novel QTM model of traffic flow with non-homogeneous time steps and show how to encode it as a linear program for simulating traffic. We proceed to allow the traffic signals to become discrete variables subject to a delay minimizing optimization objective and standard cycle and phase time constraints leading to our final MILP formulation of traffic signal control. We then experiment with this novel QTM-based MILP control in a range of networks demonstrating the improved scalability possible with non-homogeneous time steps in comparison to the best homogeneous time step. These experiments also provide near-optimal traffic control policies for larger horizons and larger networks than shown in previous implementations of MILP-based traffic signal control. [3] [4] [5]

THE QUEUE TRANSMISSION MODEL

A Queue Transmission Model (QTM) is the tuple $(\mathcal{Q}, \mathcal{L}, \vec{\Delta t}, \mathbf{I})$, where $\mathcal{Q}$ and $\mathcal{L}$ are, respectively, the set of queues and lights; $\vec{\Delta t}$ is a vector of size N representing the discretization of the simulation horizon $[0, \mathrm{T}]$ and the duration in seconds of the n-th time interval is denoted as Δt_n; and $\mathbf{I}$ is a matrix $|\mathcal{Q}| \times \mathrm{T}$ in which $I_{i,n}$ represents the flow of cars requesting to enter queue i from the outside of the network at time n.

A **traffic light** $\ell \in \mathcal{L}$ is defined as the tuple $(\Psi_\ell^{\min}, \Psi_\ell^{\max}, \mathcal{P}_\ell, \vec{\Phi}_\ell^{\min}, \vec{\Phi}_\ell^{\max})$, where:

- $\mathcal{P}_\ell$ is the set of phases of ℓ;
- $\Psi_\ell^{\min}$ ($\Psi_\ell^{\max}$) is the minimum (maximum) allowed cycle time for ℓ; and
- $\vec{\Phi}_\ell^{\min}$ ($\vec{\Phi}_\ell^{\max}$) is a vector of size $|\mathcal{P}_\ell|$ and $\Phi_{\ell,k}^{\min}$ ($\Phi_{\ell,k}^{\max}$) is the minimum (maximum) allowed time for phase $k \in \mathcal{P}_\ell$.

[2] This is not explicitly mentioned later on

[3] Paper should follow the basic progression outlined in last paragraph above. Need to be careful to maintain the thread of the story throughout the paper and the summarize it in the conclusion with the major take-home results — longer horizons and larger networks for MILP-based control!

[4] We could really use some pictures in the Intro to refer to here and subsequently – both a traffic network divided into queues, and the concept of the piecewise linear evolution of traffic flow with **non-homogeneous** (dilated) time steps, something like I had provided in my early writeup. I think these help visually explain much of the context for the paper and its approach and are critical for reviewer understanding on a time budget for reading this They may only read the first 2-3 pages and then skim!

[5] A picture is worth a 1000 words but we only pay 250, hence a 4X ROI on pictures!

A **queue** $i \in \mathcal{Q}$ represents a segment of road that vehicles traverse at free flow speed; once traversed, the vehicles are vertically stacked in a stop line queue. Formally, a queue i is defined by the tuple $(\mathrm{Q}_i, \mathrm{T}_i^{\mathrm{prop}}, \mathrm{F}_i^{\mathrm{out}}, \vec{F}_i, \vec{Pr}_i, \mathcal{Q}_i^{\mathcal{P}})$ where:

- Q_i is the maximum capacity of i;
- $\mathrm{T}_i^{\mathrm{prop}}$ is the time required to traverse i and reach the stop line;
- $\mathrm{F}_i^{\mathrm{out}}$ represents the maximum traffic flow from i to the outside of the modeled network;
- $\vec{F}_i$ and $\vec{Pr}_i$ are vectors of size $|\mathcal{Q}|$ and their j-th entry (i.e., $\mathrm{F}_{i,j}$ and $\mathrm{Pr}_{i,j}$) represent the maximum flow from queue i to j and the turn probability from i to j ($\sum_{j \in \mathcal{Q}} \mathrm{Pr}_{i,j} = 1$), respectively; and
- $\mathcal{Q}_i^{\mathcal{P}}$ denotes the set of traffic light phases controlling the outflow of queue i.

Differently than CTM (8, 13), QTM does not assume that $\Delta t_n = \mathrm{T}_i^{\mathrm{prop}}$ for all $n \in \{1, \ldots, \mathrm{N}\}$, that is, the QTM can represent non-homogeneous time intervals. The only requirement over Δt_n is that no traffic light maximum phase time is smaller than any Δt_n since phase changes occur only between time intervals; formally, $\Delta t_n \leq \min_{\ell \in \mathcal{L}, k \in \mathcal{P}_\ell} \Phi_{\ell,k}^{\max}$ for all $n \in \{1, \ldots, \mathrm{N}\}$. [6]

Traffic Flow Simulation with QTM

In this section, we present how to simulate traffic flow in a network using QTM and non-homogeneous time intervals Δt. We assume for the remainder of this section that a *valid* control plan for all traffic lights is fixed and given as parameter; formally, for all $\ell \in \mathcal{L}$, $k \in \mathcal{P}_\ell$, and interval $n \in \{1, \ldots, N\}$, the binary variable $p_{\ell,k,n}$ is known a priori and indicates if phase k of light ℓ is active (i.e., $p_{\ell,k,n} = 1$) or not on interval n.

We represent the problem of finding the flow between queues as a Linear Program (LP) over the following variables defined for all interval $n \in \{1, \ldots, \mathrm{N}\}$ and queues i and j:

- $q_{i,n} \in [0, \mathrm{Q}_i]$: traffic volume of queue i during interval n;
- $f_{i,n}^{\mathrm{in}} \in [0, I_{i,n}]$: inflow to the network via queue i during interval n;
- $f_{i,n}^{\mathrm{out}} \in [0, \mathrm{F}_i^{\mathrm{out}}]$: outflow from the network via queue i during interval n; and
- $f_{i,j,n} \in [0, \mathrm{F}_{i,j}]$: flow from queue i into queue j during interval n.

The maximum traffic flow from queue i to queue j is enforced by constraints (C1) and (C2). (C1) ensures that only the fraction $\mathrm{Pr}_{i,j}$ of the total internal outflow of i goes to j, and (C2) forces the flow from i to j to be zero if all phases controlling i are inactive (i.e., $p_{\ell,k,n} = 0$ for all $k \in \mathcal{Q}_i^{\mathcal{P}}$). If more than one phase $p_{\ell,k,n}$ is active, then (C2) is subsumed by the domain upper bound of $f_{i,j,n}$.

$$f_{i,j,n} \leq \mathrm{Pr}_{i,j} \sum_{k=1}^{|\mathcal{Q}|} f_{i,k,n} \tag{C1}$$

$$f_{i,j,n} \leq \mathrm{F}_{i,j} \sum_{p_{\ell,k,n} \in \mathcal{Q}_i^{\mathcal{P}}} p_{\ell,k,n} \tag{C2}$$

[6] **To Iain**: Maybe bring forward a small network and any other figure that would help illustrate the model and comment about it.

To simplify the presentation of remainder of the LP, we define the helper variables $q^{\text{in}}_{i,n}$ (C3), $q^{\text{out}}_{i,n}$ (C4), and t_n (C5) to represent the volume of traffic to enter and leave queue i during interval n, and the time elapsed since the beginning of the simulation until the end of interval Δt_n. [7]

$$q^{\text{in}}_{i,n} = \Delta t_n (f^{\text{in}}_{i,n} + \sum_{j=1}^{|\mathcal{Q}|} f_{j,i,n}) \tag{C3}$$

$$q^{\text{out}}_{i,n} = \Delta t_n (f^{\text{out}}_{i,n} + \sum_{j=1}^{|\mathcal{Q}|} f_{i,j,n}) \tag{C4}$$

$$t_n = \sum_{x=1}^{n} \Delta t_x \tag{C5}$$

In order to account for the misalignment of the different Δt and $\mathrm{T}^{\text{prop}}_i$, we need to find the volume of traffic that was able to arrive at queue i, traverse it (i.e., wait $\mathrm{T}^{\text{prop}}_i$ seconds), and reach the stop line before Δt_n is over. This volume of traffic is obtained by integrating over the current interval with the rate at which traffic was arriving during the interval m containing the time $t_n - \mathrm{T}^{\text{prop}}_i$, where m is the interval such that $t_m \leq t_n - \mathrm{T}^{\text{prop}}_i < t_{m+1}$. [8] The input rate of queue i during interval m is found by dividing $q^{\text{in}}_{i,m}$ with Δt_m, and then the total traffic arriving during the interval n is found by multiplying this rate by Δt_n. The flow conservation principle for non-homogeneous time steps is presented in (C6). If Δt is homogeneous for all n then (C6) reduces to $q_{i,n} = q_{i,n-1} - q^{\text{out}}_{i,n-1} + q^{\text{in}}_{i,m}$. To insure that the total volume of traffic travelling down the queue and waiting at the stop line does not exceed the capacity if the queue, we apply (C7).

$$q_{i,n} = q_{i,n-1} - q^{\text{out}}_{i,n-1} + \frac{\Delta t_n}{\Delta t_m} q^{\text{in}}_{i,m} \tag{C6}$$

$$\frac{\Delta t_n}{\Delta t_m} q^{\text{in}}_{i,m} + \sum_{k=m+1}^{n} q^{\text{in}}_{i,k} \leq \mathrm{Q}_i - q_{i,n-1} \tag{C7}$$

As with MILP formulations of CTM (e.g. Lin and Wang (*8*)), QTM is also susceptible to *withholding traffic*, i.e., the optimizer might prevent cars from moving from i to j even though the associated traffic phase is active and j is not full. We address this issue through our objective function (O1) by maximizing the total outflow $q^{\text{out}}_{i,n}$ (i.e., both internal and external outflow) of i plus the inflow $f^{\text{in}}_{i,n}$ from the outside of the network to i. This quantity is weighted by the remaining time until the end of the simulation horizon T to force the optimizer to allow as much traffic volume as possible into the network and move traffic to the outside the network as soon as possible. (O1) is analogous to minimizing delay in CTM models, e.g., (O1) is equivalent to the objective function

[7] **To Iain**: Triple check my explanation.

[8] **To Felipe**: Perhaps add this: Since the QTM is piecewise linear over an interval, the rate at which traffic enters a queue remains constant over the interval, and can be found by dividing $q^{\text{in}}_{i,m}$ by the Δt_m

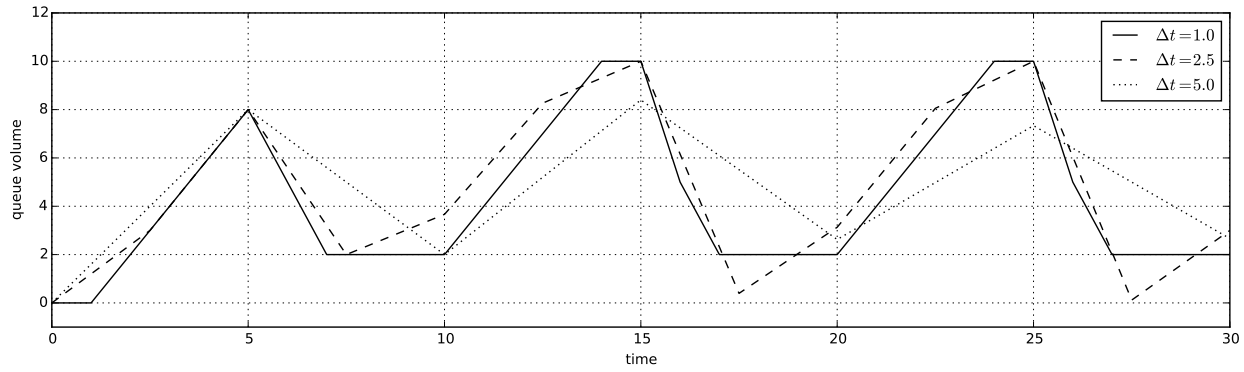

(a)

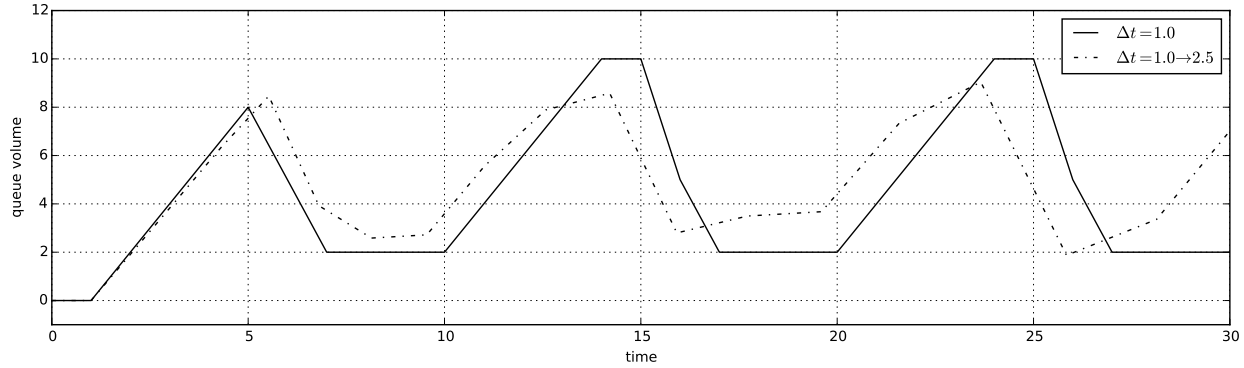

(b)

FIGURE 1 An example showing the evolution of traffic volume in a queue over time. (a) Convergce with increasing refinement of Δt from 5.0 down to 1.0. (b) Dilation of Δt from 1.0 to 2.5 compared to a fixed Δt of 1.0.

(O3) in Lin and Wang (*8*) for their parameters $\alpha = \beta = 1$. [9] [10]

$$\max \sum_{n=1}^{\mathrm{N}} \sum_{i=1}^{|\mathcal{Q}|} (\mathrm{T} - t_n + 1)(q_{i,n}^{\text{out}} + f_{i,n}^{\text{in}}) \tag{O1}$$

The objective function (O1) and constraints (C1–C7) form the LP representing the dynamic, piecewise linear model of flow in a QTM network over time when a control plan $p_{\ell,k,n}$ is given as an input parameter.

Figures 1(a), 1(a) and 2 show the results of applying the LP formulation to a simple model with a fixed signal plan, using both homogeneous $\vec{\Delta}t$ and non-homogeneous $\vec{\Delta}t$.

TRAFFIC CONTROL WITH QTM AS AN MILP

In this section, we remove the assumption that a valid control plan for all traffic lights is given and extend the LP (O1, C1–C7) to an Mixed-Integer LP (MILP) that also computes the optimal

[9] **To Iain**: Add a paragraph linking the plots with the objective function.

[10] Show diagrams with traffic predictions converging as time increment gets smaller. Validates that large time-steps are rough approximations while model behavior converges for small time steps.

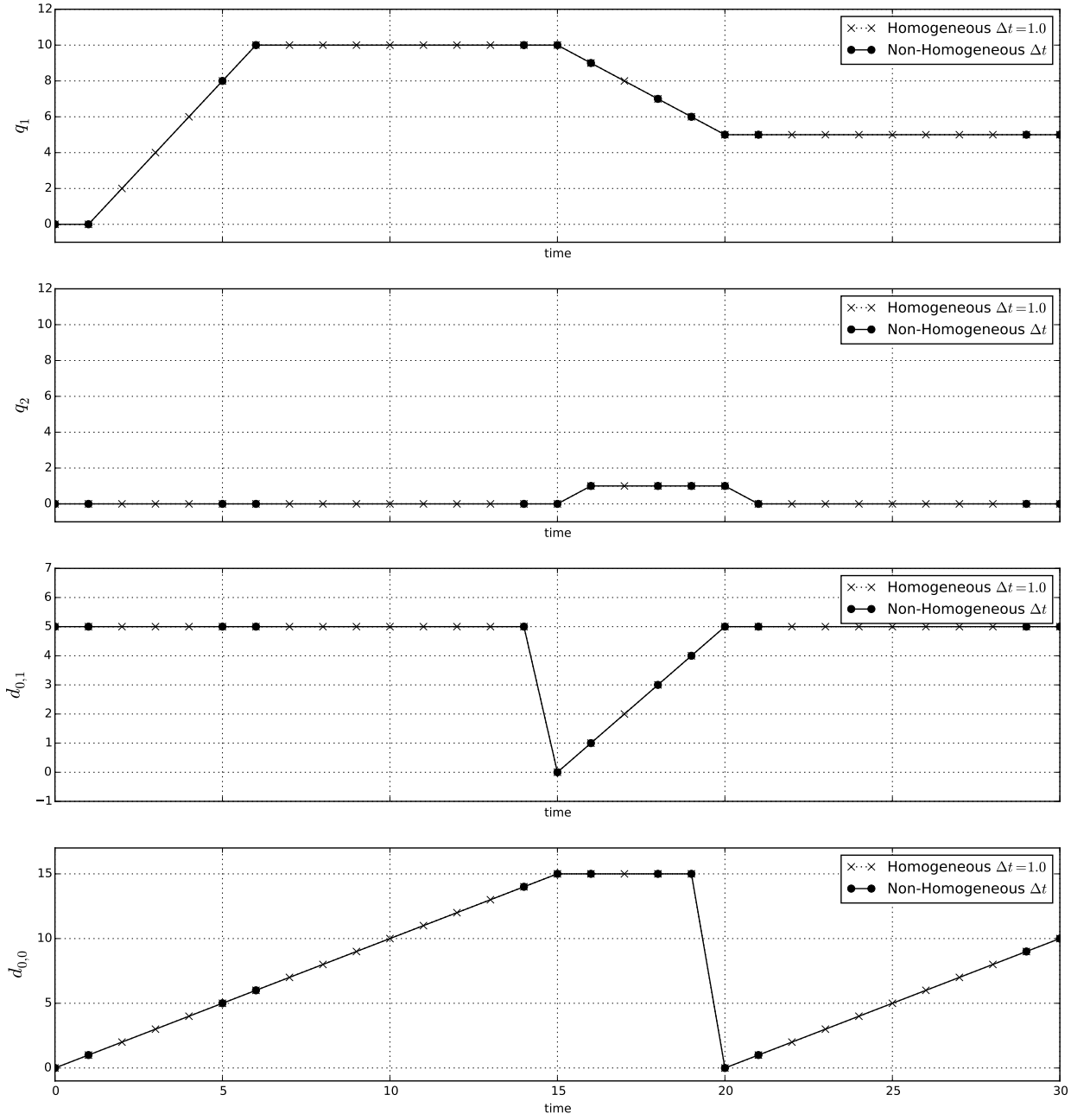

FIGURE 2 An example showing the convergence between a homogeneous solution with $\Delta t = 1.0$ and a non-homogeneous solution over 30 seconds for the same network. By using non-homogeneous time steps the same solution is found with only 14 sample points compared to 30 for homogeneous solution.

control plan. Formally, for all $\ell \in \mathcal{L}$, $k \in \mathcal{P}_\ell$, and interval $n \in \{1, \ldots, N\}$, the phase activation parameter $p_{\ell,k,n} \in \{0, 1\}$ becomes a free variable to be optimized. In order to obtain a valid control plan, we enforce that one phase of traffic light ℓ is always active at any interval n (C8) and that phase changes happen sequentially (C9), i.e., if phase k was active during interval $n - 1$ and has

become inactive in interval n, then phase $k+1$ must be active in interval n. (C9) assumes that $k+1$ equals 1 if $k = |\mathcal{P}_\ell|$. [11]

$$\sum_{k=1}^{|\mathcal{P}_\ell|} p_{\ell,k,n} = 1 \tag{C8}$$

$$p_{\ell,k,n-1} \leq p_{\ell,k,n} + p_{\ell,k+1,n} \tag{C9}$$

Next, we enforce the minimum and maximum phase durations (i.e., $\Phi^{\min}_{\ell,k}$ and $\Phi^{\max}_{\ell,k}$) for each phase $k \in \mathcal{P}_\ell$ of traffic light ℓ. To encode these constraints, we use the helper variable $d_{\ell,k,n} \in [0, \Phi^{\max}_{\ell,k}]$ defined by constraints (C10–C14) that: (i) holds the elapsed time since the start of phase k when $p_{\ell,k,n}$ is active (C10,C11) (Figure 3(a)); (ii) is constant and holds the duration of the last phase until the next activation when $p_{\ell,k,n}$ is inactive (C12,C13) (Figure 3(b)); and (iii) is restarted when phase k changes from inactive to active (C14) (Figure 3(c)). Notice that (C10–C14) employs the *big-M* method to turn the cases that should not be active into subsumed constraints based on the value of $p_{\ell,k,}$. We use $\Phi^{\max}_{\ell,k}$ as our large constant since $d_{\ell,k,n} \leq \Phi^{\max}_{\ell,k}$ and $\Delta t_n \leq \Phi^{\max}_{\ell,k}$ by assumption (Section 2.1). Similarly, constraint (C15) ensures the minimum phase time of k and is not enforced while k is still active.

$$d_{\ell,k,n} \leq d_{\ell,k,n-1} + \Delta t_{n-1} p_{\ell,k,n-1} + \Phi^{\max}_{\ell,k}(1 - p_{\ell,k,n-1}) \tag{C10}$$

$$d_{\ell,k,n} \geq d_{\ell,k,n-1} + \Delta t_{n-1} p_{\ell,k,n-1} - \Phi^{\max}_{\ell,k}(1 - p_{\ell,k,n-1}) \tag{C11}$$

$$d_{\ell,k,n} \leq d_{\ell,k,n-1} + \Phi^{\max}_{\ell,k} p_{\ell,k,n-1} \tag{C12}$$

$$d_{\ell,k,n} \geq d_{\ell,k,n-1} - \Phi^{\max}_{\ell,k} p_{\ell,k,n} \tag{C13}$$

$$d_{\ell,k,n} \leq \Phi^{\max}_{\ell,k}(1 - p_{\ell,k,n} + p_{\ell,k,n-1}) \tag{C14}$$

$$d_{\ell,k,n} \geq \Phi^{\min}_{\ell,k}(1 - p_{\ell,k,n}) \tag{C15}$$

Finally, we constrain the sum of all the phase durations for light ℓ to be within the cycle time limits $\Psi^{\min}_\ell$ (C16) and $\Psi^{\max}_\ell$ (C17) (Figure 3(d)). In both (C16) and (C17), we use the duration of phase 1 of ℓ from the previous interval $n-1$ instead of the current interval n because (C14) forces $d_{\ell,1,n}$ to be 0 at the beginning of each cycle; however, from the previous end of phase 1 until $n-1$, $d_{\ell,1,n-1}$ holds the correct elapse time of phase 1. Additionally, (C16) is enforced right after the end of the each cycle, i.e., when its first phase is changed from inactive to active. [12]

$$d_{\ell,1,n-1} + \sum_{k=2}^{|\mathcal{P}_\ell|} d_{\ell,k,n} \geq \Psi^{\min}_\ell (p_{k,1,n} - p_{k,1,n-1}) \tag{C16}$$

$$d_{\ell,1,n-1} + \sum_{k=2}^{|\mathcal{P}_\ell|} d_{\ell,k,n} \leq \Psi^{\max}_\ell \tag{C17}$$

The MILP that encodes the problem of finding the optimal traffic control plan in a QTM network is defined by (O1, C1–C17).

[11] **To Iain**: I removed the constraint $p_{\ell,k,n} + p_{\ell,k+1,n} \leq 1$ because it is subsumed by $p_{\ell,k,n} \in \{0,1\}$ and (C8)

[12] **To Iain**: Relate the phase and cycle constraints with the plots

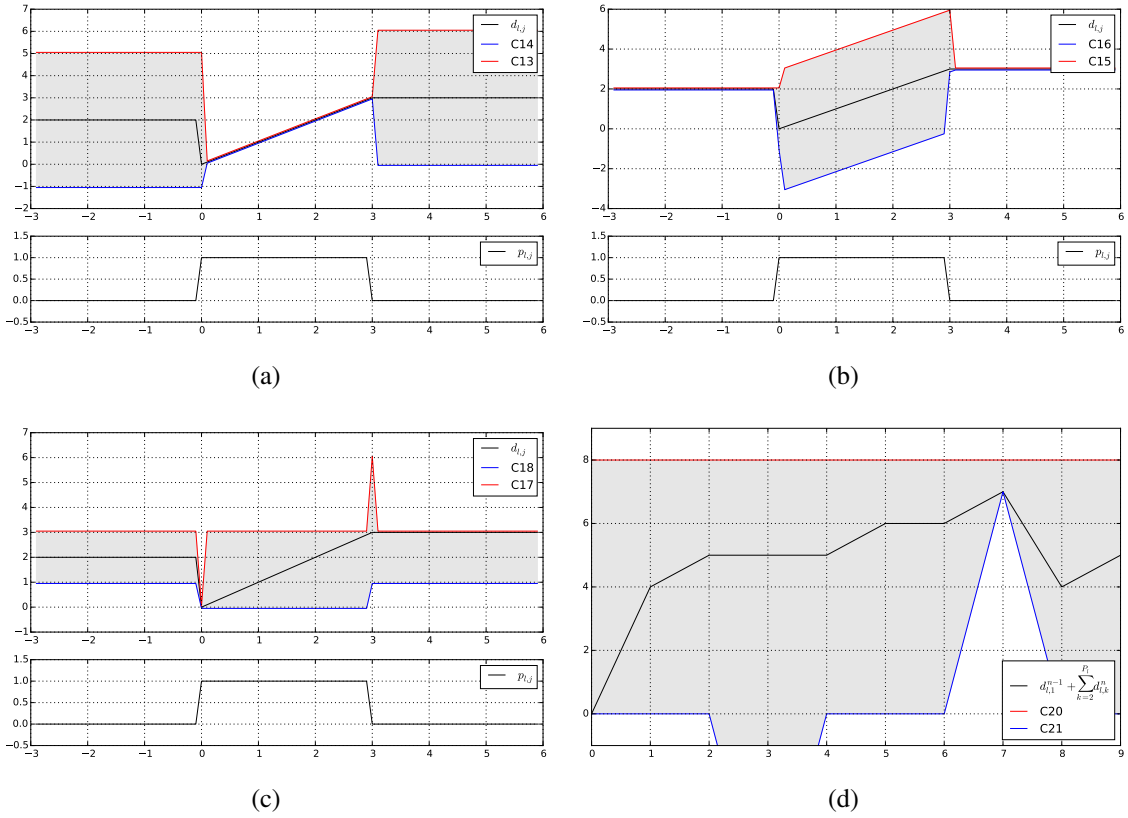

FIGURE 3 An example showing the phase and cycle time constraint envelopes. In (a), (b) and (c), $\Phi^{\min}_{\ell,k} = 1$ and $\Phi^{\max}_{\ell,k} = 3$, the duration of the previous activation was 2 and the duration of the current activation is 3. In (d), the total cycle time is 7 with $\Psi^{\min}_{\ell} = 7$, $\Psi^{\max}_{\ell} = 8$

EMPIRICAL EVALUATION

[13]

In this section we compare the performance of non-homogeneous solutions with homogeneous solutions. Our hypothesis is that an aggregate plan formed from a set of shorter planning steps, will converge on the optimum plan as the amount of look ahead at each step is increased. We then exploit the non-homogeneity of the QTM to vary $\vec{\Delta t}$ such that we sample with reducing resolution as we approach the planning horizon. Compared with a homogeneous $\vec{\Delta t}$ of the same length, the non-homogeneous solution will have a greater look ahead, but with decreasing resolution. Reducing the resolution with look ahead seems reasonable as the accuracy of the plan will also reduce over time when compared with the actual state of the network that later eventuates. [14]

Networks

To demonstrate the scalability of the QTM, we evaluate three networks of increasing complexity (Figure 5). The first consists of an avenue crossed by three side streets at controlled intersec-

[13] Start this section with the experimental rationale... what hypotheses are we trying to evaluate in this section?

[14] Add a planning horizon to the planning figure

tions. The second introduces a parallel avenue to form a grid network with a total of three controlled intersections. And the third is a more complex grid network with 9 controlled intersections between six avenues, with a seventh avenue running through at a diagonal.

The traversal time of each queue i ($\mathrm{T}_i^{\mathrm{prop}}$) in all three networks is set at 9s between intersections (a distance of about 100m with a free flow speed of 50km/h). The maximum capacity (Q_i) of each queue not leading in from the boundary of the network is set at 60 cars. For queues leading in from the boundary, the capacity is increased to buffer any spill back from the stop line and prevent interruption of the input demand profile. Flows are defined from the head of each queue i into the tail of the next queue j. There is no turning traffic ($\mathrm{Pr}_{i,j} = 1$), and in all cases the maximum flow rate between queues, $\mathrm{F}_{i,j}$, is set at 5 cars per second. Each intersection in networks 1 and 2 has two phases: North-South (NS) and East-West (EW). In network 3, lights 2, 4 and 6 have an additional Northeast-Southwest phase to control the diagonal avenue. For networks 1 and 2, $\Phi_{\ell,k}^{\min}$ is 1s, $\Phi_{\ell,k}^{\max}$ is 3s, $\Psi_{\ell}^{\min}$ is 2s, and $\Psi_{\ell}^{\max}$ is 6s, for all traffic light ℓ and phase k. For network 3, $\Phi_{\ell,k}^{\min}$ is 1s and $\Phi_{\ell,k}^{\max}$ is 6s for all ℓ and k; and $\Psi_{\ell}^{\min}$ is 2s and $\Psi_{\ell}^{\max}$ is 12s for all lights ℓ except for 2, 4 and 6 in which $\Psi_{\ell}^{\min}$ is 3s and $\Psi_{\ell}^{\max}$ is 18s.

Experimental Methodology

For each network, a background level of inflow is first established and left to run for 55s to allow the solver to settle on a stable policy. Then a spike in demand is introduced to some of the input queues for 15s to trigger a policy change, with the expectation that plans generated with longer look ahead will produce a more coordinated global policy change. The demand is then returned to the background level for another 15s before being reduced to zero, and finally sufficient time is given to allow the network to clear of traffic. By clearing the network we can easily measure the total travel time for all the traffic as the area between the cumulative arrival and departure curves measured at the boundaries of the network. Table 1 presents the demand profile of each network.

For both homogeneous and non-homogeneous intervals, we use the MILP QTM formulation (Section 3) in a receding horizon control manner: a control plan is computed for a pre-defined horizon (smaller than T) and only a prefix of this plan is executed before generating a new control plan. Our receding horizon approach is depicted in Figure 4 and we refer to the planning horizon as a major frame and its executable prefix as a minor frame. Notice that, while the plan for a minor frame is being executed, we can start computing the solution for the next major frame based on a forecast model .[15]

To perform a fair comparison between the homogeneous and non-homogeneous discretization, we fix the size of all minor frames to 10s and force it to be discretized in homogeneous intervals of 0.25s. For the homogeneous experiments, Δt is kept at 0.25s throughout the major frame and for the non-homogeneous experiments Δt linearly increases from 0.25s at the end of the minor frame through to 1.0s at the end of the major frame.[16] We analyze the effect of the major frame size by varying it from 20s through to 120s.[17] Once we have generated a series of minor frames, we concatenate them into a single plan and simulate the flow through the network using the QTM LP formulation with a fixed (homogeneous) Δt of 0.25s. [18] We also compare both receding horizon approaches against the optimal solution obtained by computing a single control plan for

[15] FWT: not sure if we should mention this.

[16] **To Iain**: Can you provide a more precise explanation? E.g., what is the rate in which it increases? *Done*.

[17] **To Iain**: What is the largest size of the major frame? *Done*.

[18] Do we need to justify why we use the QTM as the simulator over say a micro simulator?

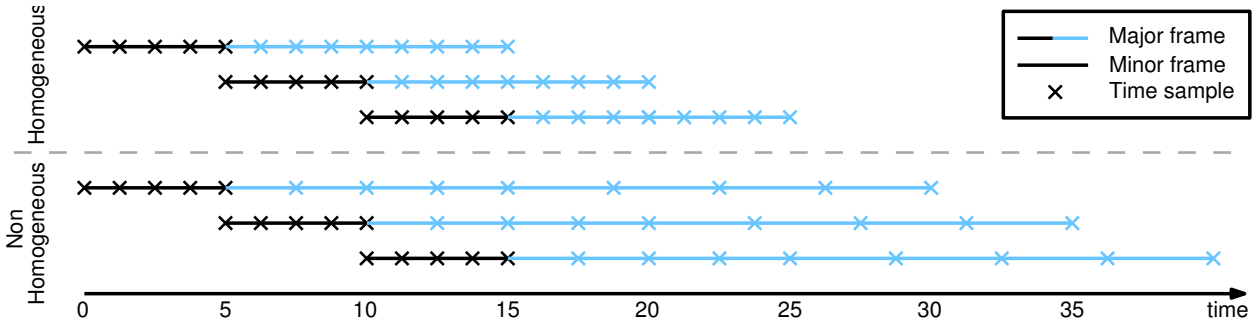

FIGURE 4 Receding horizon planning

the entire control horizon (i.e., $[0, \mathrm{T}]$) using a fixed Δt of 0.25s.

For all our experiments, we used Gurobi™ as MILP solver with 12 threads on a 3.1GHz AMD Opteron™ 4334 processor with 12 cores. We limit MIP gap accuracy to 0.1% and the time cutoff for solving a major frame to 3000s for the receding horizon approaches and unbounded for the optimal plan. [19] All our results are averaged over five runs to account for Gubori's stochastic strategies.

TABLE 1 Network Demand Profiles (vehicles per second)

	Inflow Queues	0 - 55 s	55 - 70 s	70 - 85 s	> 85 s
Network 1	q_0	1	1	1	0
	q_4, q_7	4	4	4	0
	q_1, q_{10}	2	4	2	0
Network 2	q_0	1	1	1	0
	q_4, q_7, q_{14}	4	4	4	0
	q_1, q_{10}, q_{18}	2	4	2	0
Network 3	q_0	1	1	1	0
	$q_4, q_7, q_{14}, q_{25},$	4	4	4	0
	$q_1, q_{10}, q_{18}, q_{29}, q_{36}, q_{40}, q_{44}$	2	4	2	0

Results

We compare the performance of non-homogeneous and homogeneous solutions in two ways: comparing the decrease in total travel time with increasing major frame time (greater look ahead), and analysing the distribution of delay in each queue of the network. Figures 6(a), 6(c) and 6(e) show a comparison between N, the number of time intervals [20] used in the major frame, vs the % improvement in total travel time, compared to the reference solution total travel time (0%). It can

[19] **To Iain**: Can you explain the following better and provide evidence: *while we can solve non-homogeneous major frames up to convergence in real time, we extend the solve time limit to 3000s for all test points for a fair comparison with the homogeneous test points.*. Deleted as it was not strictly true. Either we re-run scaled up on AWS with 10s solver time limit. Or we perhaps explain that 3000s shows that it could be scaled up to real time

[20] FWT: This is the first time we mention time samples, so we need to relate it with the Δt's and major frame or use something defined previously.

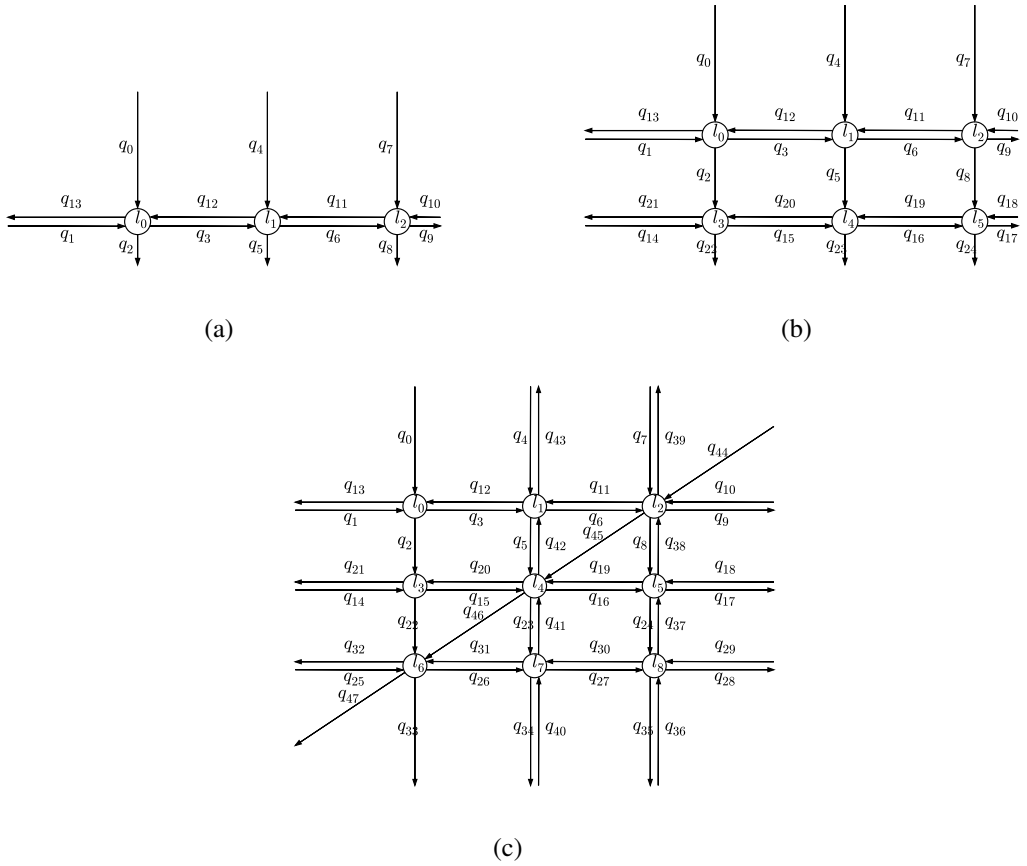

FIGURE 5 Networks used to evaluate the QTM performance.

be seen that for all three networks, using a non-homogeneous Δt converges towards the optimum total travel time more quickly than the homogeneous Δt.[21]

Figures 6(b), 6(d) and 6(f) show the distribution of the total delay observed by each car while traversing the network for different solutions. This gives us an indication of the quality of the solution in terms of the number of vehicles that experience significant delay and if the solution may be starving some parts of the network. Each group of box plots represents a different number of time samples: when the non-homogeneous Δt first converges to the optimum solution; when the homogeneous Δt first converges on the optimum solution; and the optimum solution itself. With all three networks the quality of the solution is better or the same using a non-homogeneous Δt compared to a homogeneous Δt with the same number of sample points.[22]

Finally, Figure 7 shows the cumulative arrival and departure curves and the how delay evolves over time for q_1 of network 2. Figure 7(a) shows the comparison at the point where the non-homogeneous Δt first converges and shows that with the longer major frame time of the non-homogeneous Δt, the solver is able to find a coordinated signal policy along the avenue to

[21] **To Iain**: We need to explain that as N increases, the size of the major frame increases but for a given N the major frame size between homogeneous and non-homogeneous is different. What is this relation for the non-homogeneous Δt?

[22] FWT: we need to define what we mean by better, for instance, smaller 75% quartile and max delay.

dissipate the extra traffic that arrives at the 55s point, while the homogeneous Δt with its shorter major frame fails to find a coordinated policy along the avenue and experiences more delay .[23] Once the homogeneous Δt has converged in Figure 7(b), both solutions are close to the optimum solution which is shown in Figure 7(c).

CONCLUSION

In this paper, we showed how to formulate a novel queue transmission model (QTM) model of traffic flow with non-homogeneous time steps as a linear program. We then proceeded to allow the traffic signals to become discrete variables subject to a delay minimizing optimization objective and standard traffic signal constraints leading to a final MILP formulation of traffic signal control. We experimented with this novel QTM-based MILP control in a range of networks and demonstrated that by exploiting the non-homogeneous time steps supported by the QTM, we are able to scale the model up to larger networks whilst maintaining the same quality of a homogeneous solution using more binary variables.[24] Altogether, this work represents a major step forward in the scalability of MILP-based jointly optimized traffic signal control via the use of a non-homogeneous traffic models and thus helps pave the way for fully optimized joint urban traffic signal controllers as an improved successor technology to existing signal control methods.

REFERENCES

[1] El-Tantawy, S., B. Abdulhai, and H. Abdelgawad, Multiagent reinforcement learning for integrated network of adaptive traffic signal controllers (MARLIN-ATSC): methodology and large-scale application on downtown toronto. *Intelligent Transportation Systems, IEEE Transactions on*, Vol. 14, No. 3, 2013, pp. 1140–1150.

[2] Sims, A. G. and K. W. Dobinson, SCAT–The Sydney co-ordinated adaptive traffic system: Philosophy and benefits. *IEEE Transactions on Vehicular Technology*, Vol. 29, 1980.

[3] Hunt, P. B., D. I. Robertson, R. D. Bretherton, and R. I. Winton, *SCOOT–A traffic responsive method of coordinating signals*. Transportation Road Research Lab, Crowthorne, U.K., 1981.

[4] Gartner, N., J. D. Little, and H. Gabbay, *Optimization of traffic signal settings in networks by mixed-integer linear programming*. DTIC Document, 1974.

[5] Gartner, N. H. and C. Stamatiadis, Arterial-based control of traffic flow in urban grid networks. *Mathematical and computer modelling*, Vol. 35, No. 5, 2002, pp. 657–671.

[6] Lo, H. K., A novel traffic signal control formulation. *Transportation Research Part A: Policy and Practice*, Vol. 33, No. 6, 1998, pp. 433–448.

[7] He, Q., K. L. Head, and J. Ding, PAMSCOD: Platoon-based Arterial Multi-modal Signal Control with Online Data. *Procedia-Social and Behavioral Sciences*, Vol. 17, 2011, pp. 462–489.

[23] **To Iain**: I don't think that failure to coordinate is the best way to describe it because there is coordination but it happens too late.

[24] FWT: this is the first time we make the association between number time samples and binary variables

[8] Lin, W.-H. and C. Wang, An enhanced 0-1 mixed-integer LP formulation for traffic signal control. *Intelligent Transportation Systems, IEEE Transactions on*, Vol. 5, No. 4, 2004, pp. 238–245.

[9] Han, K., T. L. Friesz, and T. Yao, A link-based mixed integer LP approach for adaptive traffic signal control. *arXiv preprint arXiv:1211.4625*, 2012.

[10] Lo, H. K., E. Chang, and Y. C. Chan, Dynamic network traffic control. *Transportation Research Part A: Policy and Practice*, Vol. 35, No. 8, 1999, pp. 721–744.

[11] He, Q., W.-H. Lin, H. Liu, and K. L. Head, Heuristic algorithms to solve 0–1 mixed integer LP formulations for traffic signal control problems. In *Service Operations and Logistics and Informatics (SOLI), 2010 IEEE International Conference on*, IEEE, 2010, pp. 118–124.

[12] Smith, S., G. Barlow, X.-F. Xie, and Z. Rubinstein, SURTRAC: Scalable Urban Traffic Control. In *Transportation Research Board 92nd Annual Meeting Compendium of Papers*, Transportation Research Board, 2013.

[13] Daganzo, C. F., The cell transmission model: A dynamic representation of highway traffic consistent with the hydrodynamic theory. *Transportation Research Part B: Methodological*, Vol. 28, No. 4, 1994, pp. 269–287.

[14] Daganzo, C. F., The cell transmission model, part II: network traffic. *Transportation Research Part B: Methodological*, Vol. 29, No. 2, 1995, pp. 79–93.

[15] Xiaojian, H., W. Wei, and H. Sheng, Urban traffic flow prediction with variable cell transmission model. *Journal of Transportation Systems Engineering and Information Technology*, Vol. 10, No. 4, 2010, pp. 73–78.

[16] Sumalee, A., R. Zhong, T. Pan, and W. Szeto, Stochastic cell transmission model (SCTM): A stochastic dynamic traffic model for traffic state surveillance and assignment. *Transportation Research Part B: Methodological*, Vol. 45, No. 3, 2011, pp. 507–533.

[17] Jabari, S. E. and H. X. Liu, A stochastic model of traffic flow: Theoretical foundations. *Transportation Research Part B: Methodological*, Vol. 46, No. 1, 2012, pp. 156–174.

[18] Huang, K. C., *Traffic Simulation Model for Urban Networks: CTM-URBAN*. Ph.D. thesis, Concordia University, 2011.

[19] Muralidharan, A., G. Dervisoglu, and R. Horowitz, Freeway traffic flow simulation using the link node cell transmission model. In *American Control Conference, 2009. ACC'09.*, IEEE, 2009, pp. 2916–2921.

[20] Gomes, G. and R. Horowitz, Optimal freeway ramp metering using the asymmetric cell transmission model. *Transportation Research Part C: Emerging Technologies*, Vol. 14, No. 4, 2006, pp. 244–262.

[21] Kim, Y., *Online traffic flow model applying dynamic flow-density relation*. Int. At. Energy Agency, 2002.

[22] Lu, S., S. Dai, and X. Liu, A discrete traffic kinetic model–integrating the lagged cell transmission and continuous traffic kinetic models. *Transportation Research Part C: Emerging Technologies*, Vol. 19, No. 2, 2011, pp. 196–205.

[23] Alecsandru, C., A. Quddus, K. C. Huang, B. Rouhieh, A. R. Khan, and Q. Zeng, An assessment of the cell-transmission traffic flow paradigm: Development and applications. In *Transportation Research Board 90th Annual Meeting*, 2011, 11-1152.

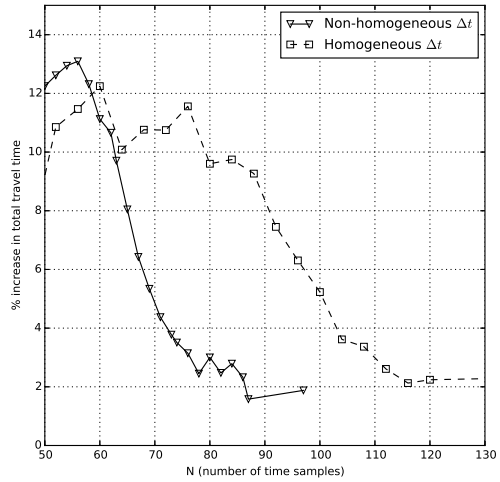

(a)

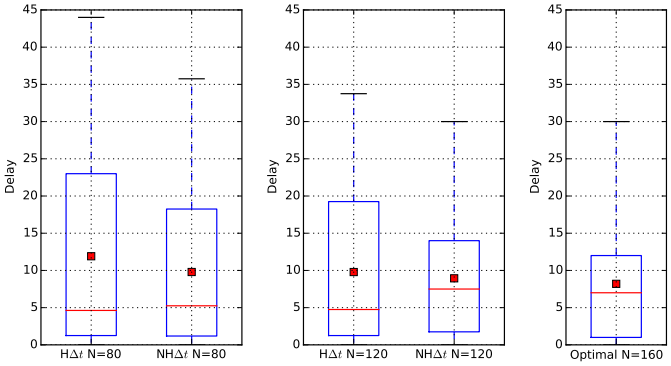

(b)

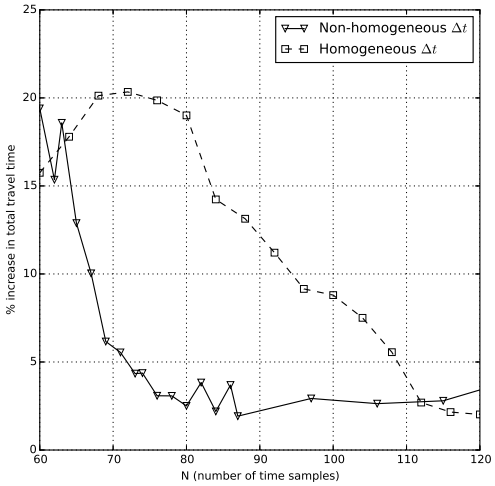

(c)

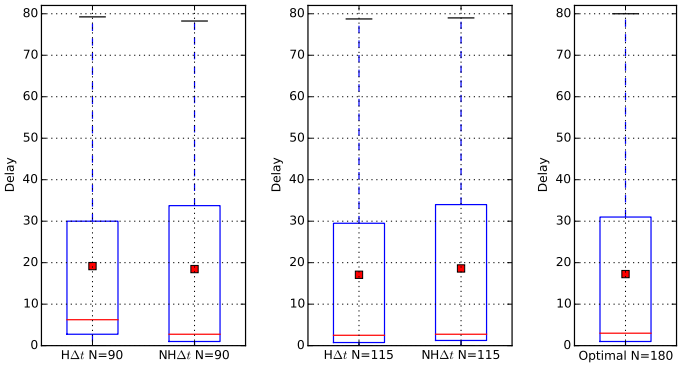

(d)

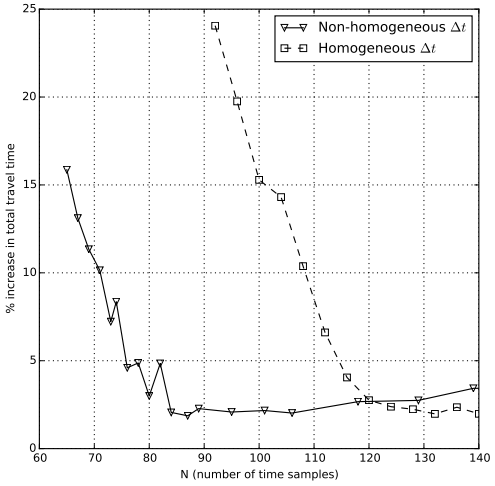

(e)

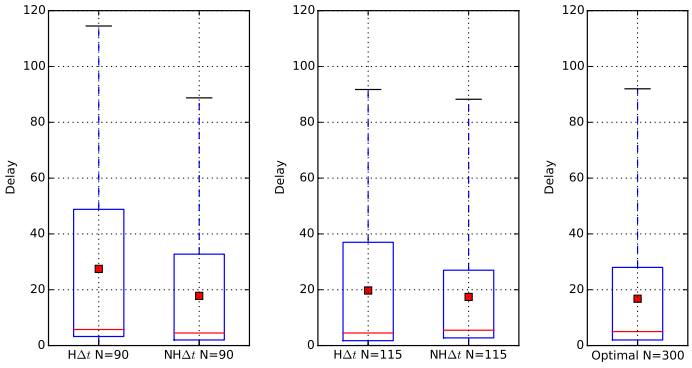

(f)

FIGURE 6 Results for the three networks showing the comparitive % increase in total travel time for the network between using a homogeneous Δt and a non-homogeneous Δt, and the distribution of delay time at the convergence point of non-homogeneous Δt, the convergence point of homogeneous Δt and for the fully solved optimal solution. (a) and (b) 3 light avenue, (c) and (d) 6 light grid, and (e) and (f) 9 light grid,

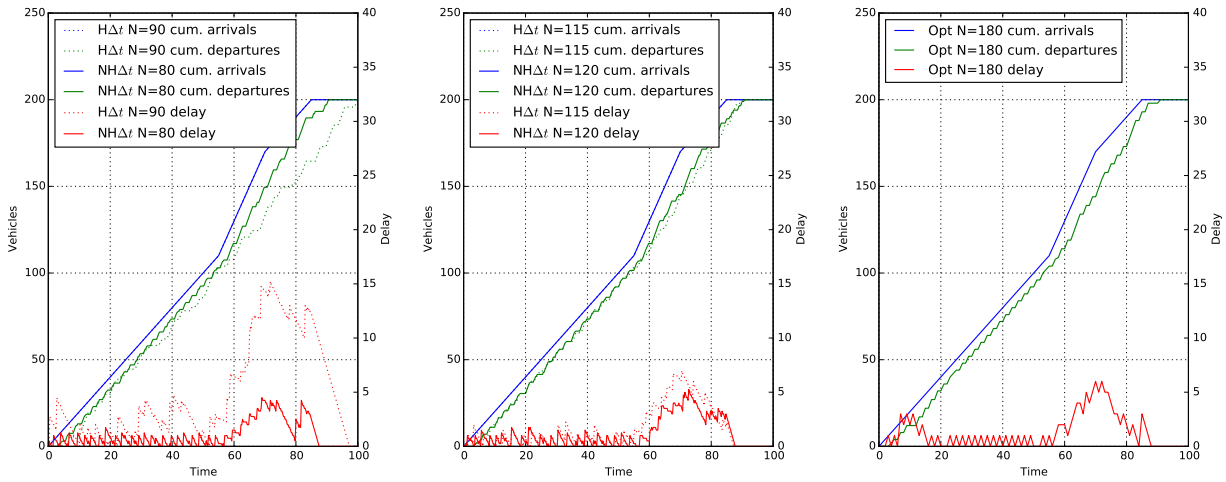

(a) (b) (c)

FIGURE 7 Cumulative arrival and departure curves and delay for queue 1 in the 6 light grid. (a) at the convergence point of the non-homogeneous Δt it is near to the optimum solution while homogeneous Δt lags behind (b) at the convergence point of homogeneous Δt both are near optimum, and (c) the fully solved optimal solution